Autoinflammatory encephalopathy due to *PTPN1* haploinsufficiency: a case series

Gaofeng Zhu, Blaise Didry-Barca, Luis Seabra, Gillian I Rice, Carolina Uggenti, Moncef Touimy, Mathieu P Rodero, Rolando Hernandez Trapero, Vincent Bondet, Darragh Duffy, Philippe Gautier, Katie Livingstone, Fraser J H Sutherland, Pierre Lebon, Mélanie Parisot, Christine Bole-Feysot, Cécile Masson, Nicolas Cagnard, Patrick Nitschké, Glenn Anderson, Birgit Assmann, Magalie Barth, Odile Boespflug-Tanguy, Felice D'Arco, Imen Dorboz, Thomas Giese, Yael Hacohen, Miroslava Hancarova, Marie Husson, Anne Lepine, Ming Lim, Maria Margherita Mancardi, Isabelle Melki, David Neubauer, Mario Sa, Zdenek Sedlacek, Angelika Seitz, Mika Shapiro Rottman, Sylvia Sanquer, Rachel Straussberg, Markéta Vlčková, Frédéric Villéga, Matias Wagner, Ayelet Zerem, Joseph A Marsh, Marie-Louise Frémond, Marios Kaliakatsos, Yanick J Crow, Marie-Thérèse El-Daher, Alice Lepelley

Lancet Neurol 2025; 24: 218–29

See Comment page 183

MRC Human Genetics Unit, Institute of Genetics and Cancer, University of Edinburgh, Edinburgh, UK (G Zhu MSc, C Uggenti PhD, R Hernandez Trapero PhD, P Gautier PhD, K Livingstone MSc, F J H Sutherland MSc, Prof J A Marsh PhD, Prof Y J Crow MD PhD, M-T El-Daher PhD); **Laboratory of Neurogenetics and Neuroinflammation, Imagine Institute, INSERM UMR1163** (B Didry-Barca MSc, L Seabra MSc, M Touimy PharmD, M P Rodero PhD, I Melki MD PhD, Prof M-L Frémond MD PhD, Prof Y J Crow, A Lepelley PhD), **Translational Immunology Unit, Institut Pasteur** (V Bondet PhD, D Duffy PhD), **Medical School** (Prof P Lebon MD), **Genomics Core Facility, Institut Imagine-Structure Fédérative de Recherche Necker, INSERM U1163 et INSERM US24/CNRS UAR3633** (M Parisot BSc, C Bole-Feysot PhD), **Bioinformatics Platform, Institut Imagine-Structure Fédérative de Recherche Necker, INSERM U1163 et INSERM US24/CNRS UMS3633** (C Masson MSc, N Cagnard MSc, P Nitschké PhD), **and Biochemistry, Metabolomics, and Proteomics Department, Necker Hospital, Assistance Publique-Hôpitaux de Paris (AP-HP) Centre** (S Sanquer PhD), **Université Paris Cité, Paris, France; Division of Evolution and Genomic Sciences, School of Biological Sciences, Faculty of Biology, Medicine, and Health, University of Manchester, Manchester Academic Health Science Centre, Manchester, UK** (G I Rice PhD); **Department of Histopathology, Camelia Botnar Laboratories** (G Anderson MSc),

Summary

Background Through the agnostic screening of patients with uncharacterised disease phenotypes for an upregulation of type I interferon (IFN) signalling, we identified a cohort of individuals heterozygous for mutations in *PTPN1*, encoding the protein-tyrosine phosphatase 1B (PTP1B). We aimed to describe the clinical phenotype and molecular and cellular pathology of this new disease.

Methods In this case series, we identified patients and collected clinical and neuroradiological data through collaboration with paediatric neurology and clinical genetics colleagues across Europe (Czechia, France, Germany, Italy, Slovenia, and the UK) and Israel. Variants in *PTPN1* were identified by exome and directed Sanger sequencing. The expression of IFN-stimulated genes was determined by quantitative (q) PCR or NanoString technology. Experiments to assess RNA and protein expression and to investigate type 1 IFN signalling were undertaken in patient fibroblasts, hTERT-immortalised BJ-5ta fibroblasts, and RPE-1 cells using CRISPR–Cas9 editing and standard cell biology techniques.

Findings Between Dec 20, 2013, and Jan 11, 2023, we identified 12 patients from 11 families who were heterozygous for mutations in *PTPN1*. We found ten novel or very rare variants in *PTPN1* (frequency on gnomAD version 4.1.0 of $<1{\cdot}25\times10^{-6}$). Six variants were predicted as STOP mutations, two involved canonical splice-site nucleotides, and two were missense substitutions. In three patients, the variant occurred de novo, whereas in nine affected individuals, the variant was inherited from an asymptomatic parent. The clinical phenotype was characterised by the subacute onset (age range 1–8 years) of loss of motor and language skills in the absence of seizures after initially normal development, leading to spastic dystonia and bulbar involvement. Neuroimaging variably demonstrated cerebral atrophy (sometimes unilateral initially) or high T2 white matter signal. Neopterin in CSF was elevated in all ten patients who were tested, and all probands demonstrated an upregulation of IFN-stimulated genes in whole blood. Although clinical stabilisation and neuroradiological improvement was seen in both treated and untreated patients, in six of eight treated patients, high-dose corticosteroids were judged clinically to result in an improvement in neurological status. Of the four asymptomatic parents tested, IFN signalling in blood was normal (three patients) or minimally elevated (one patient). Analysis of patient blood and fibroblasts showed that tested *PTPN1* variants led to reduced levels of *PTPN1* mRNA and PTP1B protein, and in-vitro assays demonstrated that loss of PTP1B function was associated with impaired negative regulation of type 1 IFN signalling.

Interpretation *PTPN1* haploinsufficiency causes a type 1 IFN-driven autoinflammatory encephalopathy. Notably, some patients demonstrated stabilisation, and even recovery, of neurological function in the absence of treatment, whereas in others, the disease appeared to be responsive to immune suppression. Prospective studies are needed to investigate the safety and efficacy of specific immune suppression approaches in this disease population.

Funding The UK Medical Research Council, the European Research Council, and the Agence Nationale de la Recherche.

Introduction

Reversible protein phosphorylation is a major cellular regulatory mechanism, with members of the protein tyrosine phosphatase (PTP) family acting to maintain homoeostatic protein tyrosine kinase signalling by removing phosphate moieties from phosphorylated substrates.[1] Phosphatases are widely expressed in the immune system, serving as key regulators of signalling in multiple types of immune cell.[2]

PTP1B, which is encoded by *PTPN1*, is a highly evolutionarily conserved, ubiquitously expressed, cytoplasmic non-receptor-type PTP.[3] *Ptpn1* knock-out mice are both viable and healthy, demonstrating enhanced insulin sensitivity and resistance to metabolic syndrome.[4]

Research in context

Evidence before this study

We searched PubMed, bioRxiv, and medRxiv for articles published in English from database inception to Aug 1, 2024, using the terms "PTPN1" and "mutation". This search showed that while somatic mutations in *PTPN1* have been described in Hodgkin lymphoma and primary mediastinal B-cell lymphoma, germline mutations have not been previously reported. We also searched the same databases using the terms "PTPN1" and "interferon" and identified reports describing variable roles for PTP1B which is encoded by *PTPN1* in the regulation of type 1 interferon (IFN) signalling in cell models.

Added value of this study

To our knowledge, our study describes for the first time the phenotypical consequences of *PTPN1* haploinsufficiency in humans. Specifically, heterozygous loss-of-function mutations in *PTPN1* are associated with a highly stereotyped neuroradiological phenotype associated with enhanced type 1 IFN signalling. Our ex-vivo and in-vitro experiments show that partial loss of PTP1B function is sufficient to impair negative regulation of type 1 IFN signalling.

Implications of all the available evidence

PTP1B is a ubiquitously expressed protein tyrosine phosphatase involved in the regulation of a broad range of signalling pathways. Our study reveals haploinsufficiency for *PTPN1* as a novel cause of disease in humans. The observed *PTPN1* variants lead to reduced levels of PTP1B and a disturbance of type 1 IFN signalling negative regulation. Notably, the associated autoinflammatory encephalopathy presents as subacute loss of motor and language skills, which may be responsive to immune suppression in some cases.

However, heterozygous somatic null variants in *PTPN1* act as driver mutations in Hodgkin lymphoma and primary mediastinal B cell lymphoma, which are associated with reduced phosphatase activity and increased phosphorylation of components of the JAK-STAT signalling pathway, indicative of loss of a negative brake on oncogenic JAK-STAT activation.[5] Of note, PTP1B has been implicated as a negative regulator of type 1 interferon (IFN) signalling[6] through various proposed mechanisms, including dephosphorylation of the tyrosine kinase TYK2 and degradation of the stimulator of IFN genes protein (STING).[7,8]

The closest paralogue to PTP1B is PTPN2, which is encoded by *PTPN2*; these proteins have a shared identity in their catalytic and substrate recognition domains, manifesting as a common activity for some substrates.[9] Notably, human germline heterozygous and biallelic variants in *PTPN2*, leading to haploinsufficiency or loss-of-function of the encoded protein, have been associated with autoimmune enteropathy,[10,11] immunodeficiency,[12] and systemic autoimmunity, including systemic lupus erythematosus and cytopenias.[12,13]

Through agnostic screening of individuals with uncharacterised disease phenotypes for an upregulation of type 1 IFN signalling, we identified a cohort of individuals heterozygous for mutations in *PTPN1*. We aimed to characterise and report the neurological disease associated with germline autosomal dominant loss-of-function mutations in *PTPN1*.

Methods

Study design and participants

In this case series, patients were identified clinically through paediatric neurologists and clinical geneticists who collaborate internationally (in Czechia, France, Germany, Italy, Israel, Slovenia, and the UK).Blood, CSF, and skin fibroblast samples for research testing were obtained from probands and parents with written informed consent. Research testing was undertaken at the UK Medical Research Council Human Genetics Unit (Institute of Genetics and Cancer, University of Edinburgh, Edinburgh, UK) and the Imagine Institute (Paris, France). Ethical approval was obtained from the Leeds (East) Research Ethics Committee (10/H1307/132) and the Comité de Protection des Personnes (ID-RCB/EUDRACT: 2014-A01017-40).

Procedures

Patients' clinical and neuroradiological data were collected, including details about clinical investigations undertaken as part of routine hospital care. Sex was defined clinically by the physician responsible for the care of the patient. In the absence of any suggestion of the existence of population founder mutations in our cohort, data on race and ethnicity were not included in this study. The clinical features of AGS1036, AGS1312, and AGS1421 were previously described by Sa and colleagues (as patients 2, 3, and 1, respectively, in that report).[14] Further details on the methods used in this study are given in the appendix (p 2).

DNA was extracted from whole blood. Exome sequencing was performed in a laboratory local to patients. Following the identification of three individuals with de-novo mutations in *PTPN1* through GeneMatcher, targeted Sanger sequencing was undertaken centrally in other patients with a similar phenotype ascertained through clinical contacts. Identified variants were assessed for their frequency in the Genome Aggregation Database (gnomAD version 4.1.0), and for their predicted effect on the encoded protein. The splicing module of Alamut Visual Plus 1.12 (Sophia Genetics; Rolle, Switzerland) was used to predict the effect of variants on splicing, and in-silico programmes (Combined Annotation Dependent Depletion [CADD] version 1.6; University of Washington, Hudson-Alpha

Department of Radiology (F D'Arco MD), **and Department of Neurology** (Y Hacohen DPhil, M Kaliakatsos PhD), **Great Ormond Street Hospital for Children, London, UK; Heidelberg University, Medical Faculty Heidelberg, Centre for Paediatric and Adolescent Medicine Department I, Division of Paediatric Neurology and Metabolic Medicine, Heidelberg, Germany** (B Assmann MD); **Service de Génétique, Centre Hospitalier Universitaire d'Angers, Angers, France** (M Barth MD); **APHP Centre de Référence LEUKOFRANCE Service de Neuropediatrie Hopital Robert Debre, Paris, France** (O Boespflug-Tanguy MD PhD, I Dorboz PhD); **Universite Paris Cité NeuroDiderot UMR INSERM 1141, Hopital Robert Debre, Paris, France** (O Boespflug-Tanguy, I Dorboz); **Institute of Immunology and German Centre for Infection Research (DZIF), Partner Site Heidelberg** (Prof T Giese MD PhD) **and Department of Neuroradiology** (A Seitz MD), **Heidelberg University Hospital, Heidelberg, Germany; Queen Square MS Centre, UCL Queen Square Institute of Neurology, Faculty of Brain Sciences, University College London, London, UK** (Y Hacohen); **Department of Biology and Medical Genetics, Charles University Second Faculty of Medicine and University Hospital Motol, Prague, Czechia** (M Hancarova PhD, Prof Z Sedlacek DSc, M Vlčková PhD); **Unité de Neurologie de l'Enfant et de l'Adolescent, CHU Pellegrin, Bordeaux, France** (M Husson MD, F Villéga MD PhD); **Service de Neuropédiatrie, Hôpital de la Timone Enfants, Marseille, France** (A Lepine MD); **Evelina London Children's Hospital, Guy's and St Thomas' NHS Foundation Trust, London, UK** (Prof M Lim PhD); **Department of Women and Children's Health, School of Life Course Sciences (SoLCS), King's College London, London, UK** (Prof M Lim); **Unit of Child Neuropsychiatry, EpiCARE Network, IRCCS Giannina Gaslini, Genova, Italy** (M M Mancardi MD PhD); **Department of General Paediatrics, Armand Trousseau Hospital, AP-HP, Sorbonne Université, Paris, France**

(I Melki); **Department of Child, Adolescent, and Developmental Neurology, University Children's Hospital, Ljubljana, Slovenia** (Prof D Neubauer MD PhD); **Department of Paediatric Neurology, Oxford University Hospitals NHS Foundation Trust, Oxford, UK** (M Sa MD); **Department of Diagnostic Imaging, Rambam Health Care Campus, Faculty of Medicine, Technion, Haifa, Israel** (M S Rottman MD PhD); **Institute of Paediatric Neurology, Schneider Children's Medical Centre of Israel, Petach Tikva, Israel** (Prof R Straussberg MD); **Faculty of Medical and Health Sciences** (Prof R Straussberg) **and Tel Aviv Sourasky Medical Center, Faculty of Medicine** (A Zerem MD), **Tel Aviv University, Tel Aviv, Israel; Institute of Human Genetics, Klinikum Rechts der Isar, School of Medicine, Technical University of Munich, Munich, Germany** (Prof M Wagner MD); **Institute for Neurogenomics, Helmholtz Zentrum München, Neuherberg, Germany** (Prof M Wagner); **Division of Paediatric Neurology, Developmental Neurology, and Social Pediatrics, Dr von Hauner Children's Hospital, Munich, Germany** (Prof M Wagner); **Pediatric Neurology Institute, Dana-Dwek Children's Hospital; Reference Centre for Inflammatory Rheumatism, Autoimmune Diseases and Systemic Interferonopathies in Children (RAISE), Paris, France** (Prof M-L Frémond); **Department of Paediatric Haematology-Immunology and Rheumatology, Necker-Enfants Malades Hospital, AP-HP, Paris, France** (Prof M-L Frémond); **Department of Neuroscience, Institute of Child Health, University College London, London, UK** (M Kaliakatsos)

Correspondence to:
Dr Yanick J Crow, MRC Human Genetics Unit, Institute of Genetics and Cancer, Edinburgh EH4 2XU, UK
yanick.crow@ed.ac.uk

or

Dr Alice Lepelley, Institute Imagine, 75010 Paris, France
alice.lepelley@inserm.fr

See Online for appendix

Institute for Biotechnology and Berlin Institute of Health at Charité, Universitätsmedizin Berlin, Germany; Sorting Intolerant From Tolerant version [SIFT] version 6.2.0; and Polymorphism Phenotyping version 2, Division of Genetics, Department of Medicine, Brigham and Women's Hospital and Harvard Medical School, Boston, MA, USA) protein modelling (using ChimeraX version 1.7.1; University of California San Francisco, CA, USA), and FoldX (Centre for Genome Regulation) were employed to predict the effect of non-synonymous missense variants on PTP1B. Inheritance was determined when parental DNA was available.

The expression of IFN-stimulated genes (ISGs) in blood was assessed either by quantitative (q)PCR or using NanoString technology (nCounter [Gene expression CodeSet]; Nanostring, a Bruker Company, Seattle, WA, USA).[15,16] IFN-α protein concentrations were measured by digital ELISA, and IFN-α activity was measured by cytopathic protection assay.[17,18] Experiments to assess RNA and protein expression and to investigate type 1 IFN signalling in the context of wildtype or mutant *PTPN1* were undertaken in patient fibroblasts, BJ-5ta hTERT immortalised fibroblasts, and hTERT RPE-1 cells using CRISPR–Cas9 gene editing and standard cell biology techniques.

Statistical analysis

Data are presented as mean (standard error of the mean [SEM]). All statistical testing was undertaken in GraphPad Prism 10. For comparison between two groups, an unpaired *t* test or ratio paired *t* test was chosen when appropriate (as indicated in figure legends). For comparison among three or more groups of the same categorial variable (ie, genotype in this Article), one-way ANOVA was used. For comparison among three or more groups of two independent categorical variables (ie, genotype and treatment in this Article), mixed-model two-way ANOVA was adopted. p values are annotated in each graph; more details are in the appendix (p 5). For RNA sequencing analysis with DESeq2 (version 1.46.0 in R version 4.3.3), the adjusted p values were obtained by the Wald test, with Benjamini and Hochberg correction for multiple comparisons. In gene-set enrichment analysis, nominal p values were calculated using an empirical gene set-based permutation test, and false discovery rate was adjusted for gene-set size and multiple hypotheses testing; more details are in the appendix (p 5).

Role of the funding source

The funders of the study had no role in study design, data collection, data analyses, data interpretation, or writing of the report.

Results

Between Dec 20, 2013, and Jan 11, 2023, as part of an ongoing research strategy in Edinburgh, UK (MRC Human Genetics Unit) and Paris, France (Imagine Institute) involving the agnostic screening of patients with uncharacterised disease phenotypes for an upregulation of type 1 IFN signalling, a male child was identified (designated AGS761) who experienced infantile-onset subacute loss of motor and language skills and who was found to carry a de-novo63+1G→C canonical donor splice site in intron 1 of *PTPN1* (table 1). Using GeneMatcher, a further two patients were identified (at centres in France and Czechia) with de-novo variants in *PTPN1*: the first was a patient (AGS2942) with a 466C→T transition predicted to result in a STOP mutation (Arg156Ter); and the second was a patient (AGS3148) with a 154+1del canonical donor splice site variant in intron 2. Through collaboration with international colleagues, a further nine patients were

	cDNA variant of *PTPN1*	Consequence in PTP1B	Inheritance	Allele frequency (gnomAD version 4.1.0)
AGS492.1 and AGS492.4	590A→G (exon 6)	Lys197Arg*	Paternally inherited (in two cousins)†	0
AGS761	63+1G→C (intron 1)	Partial intron 1 retention and NMD	De novo	0
AGS1036	466C→T (exon 5)	Arg156Ter‡	Maternally inherited	0
AGS1312	1000delG (exon 8)	Val334Ter	Paternally inherited	0
AGS1421	370_386del (exon 5)	Tyr124ArgfsTer7	Paternally inherited	0
AGS2942	466C→T (exon 5)	Arg156Ter‡	De novo	0
AGS3148	154+1del (intron 2)	Exon 2 skipping	De novo	0
AGS3165	784C→T (exon 7)	Gln262Ter	Maternally inherited	0
AGS3479	166C→T (exon 3)	Arg56Trp*‡	Maternally inherited	2/1 612 624 alleles
AGS3542	505C→T (exon 6)	Arg169Ter	Paternally inherited	1/1 613 702 alleles
AGS3561	619G→T (exon 6)	Glu207Ter	Paternally inherited	0

NMD=nonsense-mediated decay. *Lys197 and Arg56 have been reported as non-catalytic residues which might alter the function of the catalytically active site (ie, allosteric regulation) of PTP1B function.[19,20] †Two first cousins related through their unaffected fathers. ‡Arg56Trp and Arg156Ter mutations have been reported as somatic mutations in Hodgkin lymphoma and primary mediastinal B cell lymphoma, respectively.[5]

Table 1: **Summary of molecular data, by family, for each patient identifier**

identified who were heterozygous for mutations in *PTPN1*. Six probands had mutations in *PTPN1* that were predicted to introduce a premature STOP mutation in PTP1B (Tyr124ArgfsTer7 [AGS1421], Arg156Ter [AGS1036], Arg169Ter [AGS3542], Glu207Ter [AGS3561], Gln262Ter [AGS3165], and Val334Ter [AGS1312]). Two probands had mutations that involved canonical splice-site nucleotides likely to disrupt mRNA splicing and severely affect protein sequence (Arg56Trp [AGS3479] and Lys197Arg [AGS492.1 and AGS492.4, these two affected individuals were first cousins]). Although the two missense substitutions were predicted to have relatively mild effects on protein stability, they occurred at evolutionarily conserved residues that have been described as having important roles in the allosteric regulation of PTP1B function (figure 1B, C; appendix p 14). In total, ten novel or very rare mutations in *PTPN1* were reported in 12 symptomatic patients from 11 families (Arg156Ter being seen in two families and Lys197Arg present in two affected first cousins from one family; figure 1A; table 1). Nine family members who were identified to be asymptomatic carriers of a mutation in *PTPN1* (aged between 34 years and 52 years) did not report any significant past medical history.

PTPN1 is a highly constrained gene (constraint score [pLI] of 1 in gnomAD version 4.1.0), indicating strong negative selection against loss-of-function variants. Consistent with this background, of the variants recorded in our cohort, only Arg56Trp and Arg169Ter were present in gnomAD v4.1.0 (seen in the heterozygous state twice for Arg56Trp and once for Arg169Ter, out of >1 600 000 alleles; table 1). Although in three patients the variant appeared to have occurred de novo, in nine cases the variants were inherited from an asymptomatic parent (with two asymptomatic fathers to the two affected first cousins in family AGS492; figure 1A). It is of note that the Arg156Ter mutation was seen to occur de novo in one family (AGS2942) and to have been inherited from an asymptomatic mother in another (AGS1036; figure 1A). Of further note, the Arg156Ter mutation was previously reported as a somatic driver mutation in primary mediastinal B-cell lymphoma and the Arg56Trp mutation as a driver of Hodgkin lymphoma.

The clinical phenotype of the 12 symptomatic patients was remarkable for the high degree of stereotypy observed (table 2; appendix p 6, 20). All 12 patients experienced subacute loss of skills (age range 15 months to 8 years). Initial development was normal for 11 patients; the remaining patient demonstrated mild motor delay (did not walk independently until 21 months of age). All 12 patients demonstrated weakness and spasticity (initially manifesting as hemiparesis in seven patients, then becoming bilateral) with or without dystonia, and 11 patients exhibited bulbar involvement (dysphagia with or without dysphasia) in the absence of seizures (although noting that one patient had a febrile seizure 1 month before the onset of loss of skills). In four patients, fever and raised liver enzymes were noted around the time of presentation.

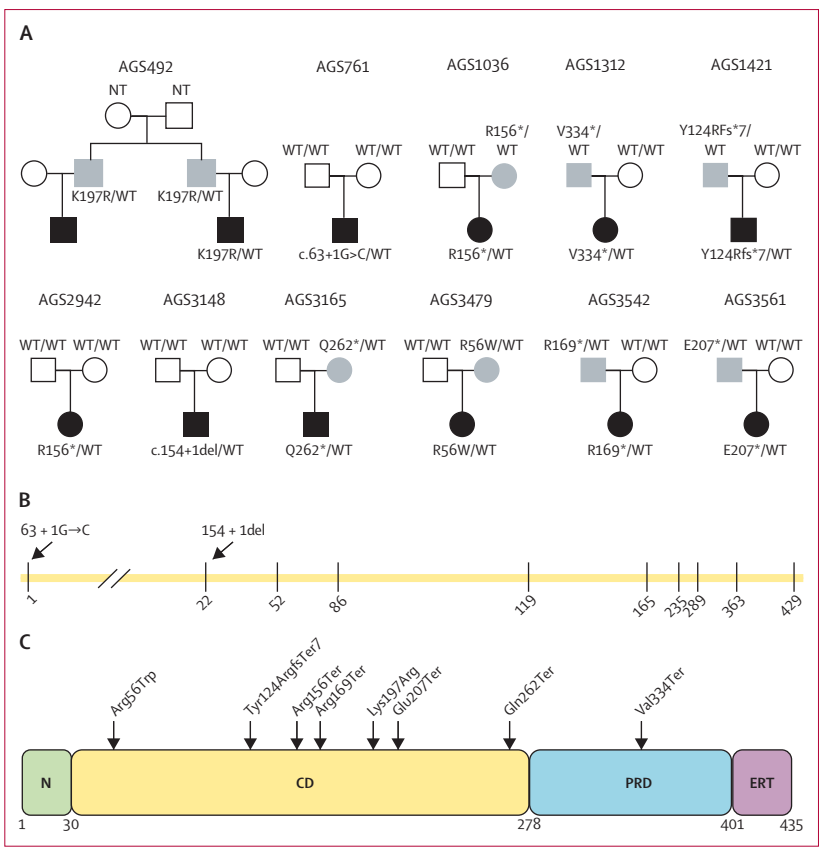

Figure 1: **Genetic data**
(A) Family pedigrees showing affected individuals with a novel or very rare heterozygous non-synonymous mutation in *PTPN1*. Circles indicate females and squares males. Black symbols denote affected mutation-positive individuals, grey symbols denote clinically asymptomatic mutation-positive individuals, and white symbols denote unaffected family members. (B) *PTPN1* locus with perpendicular lines indicating exons; numbers below the locus indicate the first amino acid position in the respective exon. The two splicing variants are depicted above the locus, with arrows showing the relative position next to the exon. (C) Protein domains of PTP1B, with amino acid numbering below. STOP mutations and non-synonymous missense substitutions are indicated. NT=not tested. WT=wildtype. N=N-terminal domain. CD=catalytic domain. PRD=proline-rich domain. ERT=Endoplasmic reticulum-targeting domain.

Cerebral atrophy was the major neuroradiological feature in nine patients, which was initially unilateral in four; non-specific white-matter changes were seen in eight individuals; intracranial calcification was reported in two patients (figure 2). Four patients underwent brain biopsy, demonstrating non-specific inflammation in three (appendix p 20).

All 12 patients had subsequent clinical stabilisation and were alive at last contact (age range 3–20 years; table 2). Seven children had severe-to-profound motor and communication difficulties (Gross Motor Function Classification System [GMCFS] and Communication Function Classification System.

[CFCS] ≥4). Two patients returned to (AGS2942) or close to (AGS1036) predisease levels of function. In eight cases, brain imaging showed complete or near-complete

resolution of the cerebral atrophy and white-matter disease seen in the initial stages of the disease.

Eight of 12 patients received immunosuppression. Clinical stabilisation and neuroradiological improvement were seen in both treated and untreated patients. However, in six of the eight patients who were treated with immunosuppressants, the improvement in neurological status was judged clinically to be probably related to immune suppression with high-dose corticosteroids, with one patient (AGS3542) showing an apparent steroid dependency over more than 2 years (table 2; appendix pp 6, 20; videos of AGS1036, AGS1312, and AGS1421 before and after treatment are available in the case study by Sa and colleagues'[19] as video 2, video 3, and video 1, respectively). Of note, clinical improvement following treatment was associated with normalisation of

	Sex	Age at onset	Clinical features	Neuroradiology (age in months at which the signs were observed)	Treatment effect	Status (GMFCS30 and CFCS31 at last contact)
AGS492.1	Male	2·5 years	Rapid onset of left-sided hemiparesis evolving to spastic dystonia tetraparesis over several months, becoming unable to sit without support and poor head control; no information on head circumference	Bilateral white-matter disease (31 months); basal ganglia calcification (31 months); repeat MRIs showed slight progression of white-matter disease (40 months; 44 months); no further follow-up imaging available	No clear improvement with oral prednisolone (1 mg/kg/day for 3 months) given at age 3 years 9 months	Condition stabilised; alive aged 11 years (GMFCS V and CFCS IV)
AGS492.4	Male	3·5 years	Rapid onset of right-sided weakness evolving to bilateral spasticity, loss of walking, dysphasia, and dysphagia over several weeks; head circumference 25th centile	White-matter disease left right with basal ganglia calcification (44 months); more profuse white-matter disease with cerebral atrophy (46 months); marked improvement in white-matter signal (96 months)	Methylprednisolone (30 mg/kg for 3 days repeated monthly for 3 months) started in first few weeks after presentation, associated with resumption of limited ambulation and less drooling	Condition stabilised; alive age 8 years (GMFCS III and CFCS IV)
AGS761	Male	15 months	Fever with irritability and rapid loss of motor skills, language, and swallowing (requiring gastrostomy) over days, becoming spastic dystonia with truncal hypotonia; raised LFTs at presentation; head circumference ninth centile	Patchy white-matter disease and cerebral atrophy (16 months)	Intravenous immunoglobulin for 6 months with no obvious effect	Condition stabilised; alive aged 8 years (GMFCS V and CFCS IV)
AGS1036; patient 2 in Sa and colleagues[14]	Female	5 years	Subacute onset over 3 months of left-sided weakness, frequent falls, and difficulties climbing stairs, also becoming dysarthric with dysphagia and drooling; subsequent spastic dystonia lower limbs worse than upper limbs, and left worse than right; normal head circumference; raised LFTs at presentation	Cerebral atrophy (right > left; 5 months after symptom onset); MRI 23 months after treatment initiation (35 months after symptom onset) showed significant reversal of cerebral atrophy	Intravenous methylprednisolone (4 courses 30 mg/kg/day for 5 days) and intravenous immunoglobulin (2 g/kg 3–4 months apart), started 12 months after symptom onset associated with significant improvement in all domains; residual lower-limb hypertonia	Condition stabilised; alive aged 13 years (GMFCS I and CFCS I)
AGS1312; patient 3 in Sa and colleagues[14]	Female	4 years	Mild motor delay (walked 21 months) then progressive loss of walking leading to use of wheelchair outside and complete loss of expressive language over 1 year with dysphagia; spastic dystonia right worse than left; head circumference <0·4th centile (no previous measures); marked improvement in lower limb tone associated with treatment, regained independent ambulation, albeit with a spastic paraplegia, and speech and swallowing returned to normal; raised LFTs at presentation	Mild global cerebral atrophy (9 months after symptom onset); MRI 13 months after treatment initiation (and 30 months after symptom onset) showed complete normalisation	Improved with intravenous methylprednisolone (3 days, 30 mg/kg/day) and intravenous immunoglobulin (2 g/kg for five courses over 20 months), started 15 months after symptom onset	Condition stabilised; alive aged 12 years (GMFCS II and CFCS I)
AGS1421; patient 1 in Sa and colleagues[14]	Male	22 months	Progressive left-sided hemiparesis extending bilaterally with spastic dystonia (lower limbs > upper limbs) over months, associated with fever, loss of speech, and dysphagia; head circumference normal; raised LFTs at presentation	Right cerebral hemiatrophy (~27 months) extending bilaterally (34 months) (12 months after symptom onset); MRI normal (76 months) (26 months after treatment)	Improved fine motor and non-verbal skills with 6 weekly intravenous methylprednisolone (30 mg/kg/day) and intravenous immunoglobulin (2 g/kg), started 18 months after symptom onset	Condition stabilised; alive aged 11 years (GMFCS IV and CFCS III)
AGS2942	Female	8 years	Appearance of left lower-limb spasticity when running, followed by cognitive decline, dysarthria, and recurrent fevers over 1 year; subsequently regained all skills; normal head circumference	Modest white-matter disease and cerebral atrophy (114 months); normalisation of cerebral atrophy and reduction of white-matter disease (125 months)	Not treated	Condition stabilised and almost returned to premorbid state; alive aged 10 years (GMFCS I and CFCS I)

(Table 2 continues on next page)

	Sex	Age at onset	Clinical features	Neuroradiology (age in months at which the signs were observed)	Treatment effect	Status (GMFCS30 and CFCS31 at last contact)
(Continued from previous page)						
AGS3148	Male	15 months	Febrile seizure followed 1 month later by loss of walking and speaking abilities so that by age 19 months speech was completely absent; he could not walk, was tetraspastic, and demonstrated bulbar involvement (dysphagia); head circumference 25–50th centile	White-matter T2 high signal (16 months); reduction (33 months) and almost normalisation of white-matter disease (168 months)	Not treated	Condition stabilised; alive aged 20 years (GMFCS V and CFCS IV)
AGS3165	Male	4·5 years	Febrile episode followed by irritability, spasticity, dysarthria, and dysphagia progressing rapidly so that within 6 months he was unable to walk; speech was incomprehensible and unsafe to swallow; normal head circumference	Normal MRI (54 months); white matter disease right left (58 months); white-matter disease more diffuse (58 months); almost complete resolution of white-matter disease (61 months)	Bolus corticosteroids (1 mg/kg/day) aged 58 months without major clinical benefit; further corticosteroid (1 mg/kg/day) aged 63 months associated with a definite improvement in walking, albeit with spastic dysplasia, speech, and swallowing	Condition stabilised; alive aged 7 years (GMFCS II and CFCS II)
AGS3479	Female	18 months	Left-sided hemiparesis progressing to four-limb spastic dystonia with dysphagia and complete loss of speech; head circumference 25th centile (75th centile 12 months earlier)	Initial right cerebral hemiatrophy (19 months); atrophy becoming bilateral in the absence of any white-matter disease (22 months); no further imaging undertaken	Intravenous immunoglobulin stopped almost immediately due to an allergic reaction; no further treatment initiated	Condition stabilised; alive aged 3 years (GMFCS V and CFCS V)
AGS3542	Female	23 months	Progressive spastic tetraparesis (left worse than right) with preserved cognition and speech, experiencing a further period of regression at age 36 months also affecting speech and swallowing; now has <20 words but communicates well with a computer and can use an electric wheelchair unassisted; normal head circumference	Initial right cerebral hemiatrophy with subtle white-matter disease left worse than right (26 months); extending bilaterally (44 months); almost normalised brain volume (60 months; 92 months)	Definite response to pulsed methylprednisolone 20 mg/kg/day for 5 days monthly for 3 months, starting at age 27 months; response to a further dose (20 mg/kg/day for 3 days per week for 4 weeks) at ages 38 months, 51 months, and beyond, because of clinical deterioration	Condition stabilised; alive aged 8 years (GMFCS IV and CFCS III)
AGS3561	Female	7 years	Appearance over several weeks of gait and speech disturbance with mild cognitive decline, evolving to spastic dystonia right worse than left with dysarthria and dysphagia; subsequently judged to show reattainment of some skills, now able to speak in simple sentences and can walk independently over short distances; normal head circumference	White-matter disease with cerebral atrophy (92 months); cerebral atrophy becoming more prominent (96 months); no further follow-up imaging available	Not treated	Condition stabilised with some reattainment of skills; alive aged 10 years (GMFCS II and CFCS II)

GMFCS=gross motor function classification system. CFCS=communication function classification system. LFTs=liver function tests.

Table 2: **Individuals' age at onset, clinical features, neuroradiology, treatment effect, and status at last contact, for each patient identifier**

ISG expression in whole blood in two of these patients (AGS1036 and AGS1421; appendix pp 14, 21).

CSF levels of neopterin—a marker of CNS inflammation that is raised consistently in type 1 interferonopathies involving the neurological system—were elevated in ten patients who were tested (range 2–45 multiples of laboratory-specific upper limits of normal; appendix p 21). Further, all 12 patients demonstrated enhanced IFN signalling, with upregulation of ISGs in whole blood on at least one occasion. Overall, 24 (83%) of 29 such results were abnormal (figure 3; appendix p 21), with serial testing revealing a fall of ISGs over time, consistent with the observed clinical stabilisation. A marked increase of IFN-α protein in CSF and serum was also recorded in one patient, and increased IFN-α activity in CSF was noted in two patients on each occasion tested (appendix p 21). Additionally, tubuloreticular inclusions—subcellular structures located within the cisternae of the endoplasmic reticulum, a marker of enhanced IFN signalling—were observed in the brain biopsy sample from AGS1036 (appendix p 14). Of four asymptomatic parents who had a mutation in *PTPN1*, IFN signalling was normal in three and minimally elevated in one (appendix p 6).

Consistent with the genetic data, reduced expression was recorded of *PTPN1* mRNA (figure 4A), and of encoded PTP1B protein (figure 4B), in the three patient fibroblast cell lines that were available and in which a predicted nonsense mutation in *PTPN1* was present. Of note, Arg156Ter was previously shown to be unstable when expressed in HEK293 cells in a study of lymphoma. *PTPN1* mRNA expression was apparently preserved in the patient with the 154+1del canonical donor splice-site variant in intron 2 (figure 4A). Indeed, deep sequencing of captured *PTPN1* cDNA from primary fibroblasts of this patient revealed skipping of exon 2 in 50% of transcripts (8036 reads versus 7931 reads for the

canonically spliced transcript), suggesting preserved expression of the mutant allele and the absence of nonsense-mediated decay (NMD; appendix p 14). However, the skipping of exon 2 leads to a frameshift and introduction of a premature stop codon in exon 3 after 19 amino acids. The putative translated peptide would have a size of 40 amino acids and 4·6 kDa (appendix p 14). Deep sequencing also revealed a transcript that used an alternative splicing site in exon 2 (2668 reads; appendix p 14) with a premature stop codon immediately downstream, leading to a putative peptide of 46 amino acids. We could not detect either truncation by western blotting of primary fibroblast lysates, a finding consistent with protein instability and the observed reduced protein expression (figure 4B). By contrast, on sequencing of *PTPN1* cDNA captured from whole blood in the patient with the 63+1G→C variant, fewer reads were observed (5122 reads for the 63+1G→C variant versus 9723 reads in a control sample) and no major splicing defect was seen, indicative of NMD of the mutated allele (appendix p 14). A novel minor splicing site was also observed in intron 1 (appendix p 14), which could lead to retention of part of intron 1, a premature stop codon and the production of a 114 amino acid peptide (appendix p 14).

Given evidence of enhanced type 1 IFN signalling in patient blood, CSF, and brain tissue, IFN signalling was tested in patient fibroblasts in vitro. On stimulation with IFNα2b, higher levels of phosphorylated STAT1 (p-STAT1) were detected compared with control fibroblasts (figure 4C). The link between loss of PTP1B

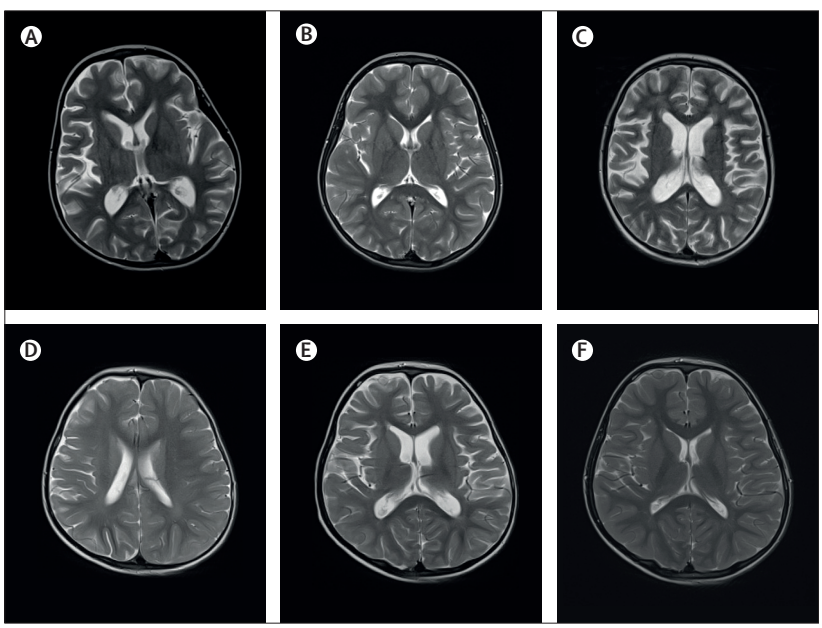

Figure 2: **Axial T2 cerebral MRIs representative of patients in the study**
(A) AGS1036 (age 5 years) 5 months after symptom onset, showing generalised volume loss more evident in the right cerebral hemisphere. (B) AGS1036 (age 8 years) at 35 months after symptom onset and 23 months after initiation of treatment, showing almost complete normalisation of the changes seen initially. (C) AGS2942 (age 9 years) showing significant corticosubcortical atrophy with passive enlargement of the ventricles and cerebral sulci, and some hypersignal of the deep white matter frontally. (D) AGS3542 (age 2 years 2 months) showing right-sided hemiatrophy and non-specific hypersignal of the deep white matter. (E) AGS3542 (age 3 years 8 months) showing bilateral atrophy. (F) AGS3542 (age 7 years 8 months) showing normalised brain volume without significant asymmetry and normalised white matter.

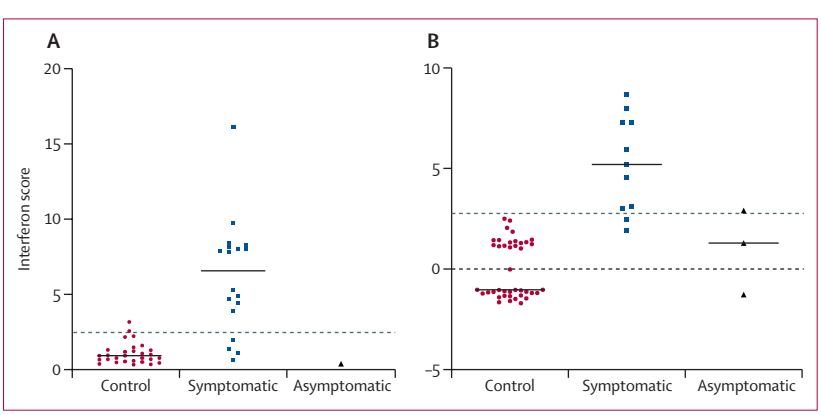

Figure 3: **Interferon expression in symptomatic patients and asymptomatic parents**
Interferon scores (median fold expression of a panel of interferon-stimulated genes) recorded in 12 symptomatic patients and four of their asymptomatic parents carrying a mutation in *PTPN1*. In families AGS492, AGS761, AGS1036, AGS1312, and AGS1421, IFN scores were derived using a six interferon-stimulated gene panel measured by qPCR (A),[15] whereas in families AGS2942, AGS3148, AGS3165, AGS3479, AGS3479, and AGS3561, a 24 interferon-stimulated gene panel was generated using NanoString technology (B).[16] The upper range of normal is calculated as +2 SD above the mean of the control group, as indicated by the dotted lines. Solid lines indicate mean; black symbols indicate individual interferon scores. qPCR=2.466. NanoString=2.758. Black lines indicate the median values for the respective groups.

Figure 4: **Studies of patient-derived primary fibroblasts and *PTPN1* deficient cells**
qPCR analysis of *PTPN1* mRNA expression (A), and representative immunoblots of PTP1B protein expression (B), in patient-derived primary dermal fibroblasts carrying the indicated heterozygous variants. For qPCR, 5–7 experiments and one-way ANOVA with Fisher's least significant difference test was used to compare the expression levels of *PTPN1* in healthy control cells and patient cells. Circles represent biological replicates, bars the means of biological replicates, and error bars the standard error of the mean. For controls, one circle represents the average for two to three HDF lines in each independent experiment. (C) Representative immunoblot of p-STAT1, STAT1, and loading control vinculin in lysates of primary fibroblasts stimulated for 15 min with IFNα2b (left), and quantification of p-STAT1 signal over vinculin signal (right). Three experiments and mixed model with Dunnett's multiple comparison test was performed. Circles represent biological replicates, bars the means of biological replicates, and error bars the standard error of the mean. For controls, one circle represents the average of two to three HDF lines in each independent experiment. (D–F) qPCR analysis of the expression of five representative ISGs (*IFI27*, *IFI44L*, *MX1*, *OAS1*, and *RSAD2*), with an ISG score calculated as the median of the expression of these genes in BJ-5ta human fibroblast cell clones WT, KO (D), WT-KO (E), or WT-KI for the 63+1G→C nucleotide substitution (F). Each circle or triangle (D–F) represents the average ISG score from independent clones of the same genotype (WT, two to four clones; WT-KO, four clones; and WT-KI, one clone) in one experiment. Bars represent the means of biological replicates, and error bars the standard error of the mean. ISG score was calculated as previously. Unpaired *t* test (D-F) was used to compare the baseline ISG expression levels in WT and mutant BJ-5ta clones. (G) qPCR of baseline ISG expression on a *PTPN1* WT or KO background in hTERT RPE-1 cells, and either WT or single KO of *IFNAR1* or *STING1*. (H) qPCR of baseline ISG expression on a *PTPN1* WT or KO background in hTERT RPE-1 cells, and cells WT or double KO for *IFNAR1* and *STING1*. ISG score is calculated as the median of the expression of four ISGs, *IFI27*, *IFI16*, *MX1* and *IRF7*. Three to four experiments and one-way ANOVA (G–H) was used to compare the levels of baseline ISG expression in the indicated genotypes. Each circle denotes the ISG score in RPE-1 cells with a distinct genotype in one independent experiment, bars represent the means of biological replicates, and error bars the standard error of the mean. HDF=control human dermal fibroblasts. IFN=interferon. ISG=IFN-stimulated genes. KO=knockout. p-STAT1=phosphorylated STAT1. qPCR=quantitative PCR. WT=wildtype. WT/KI=wildtype/knock-in. WT/KO=wildtype/knockout.

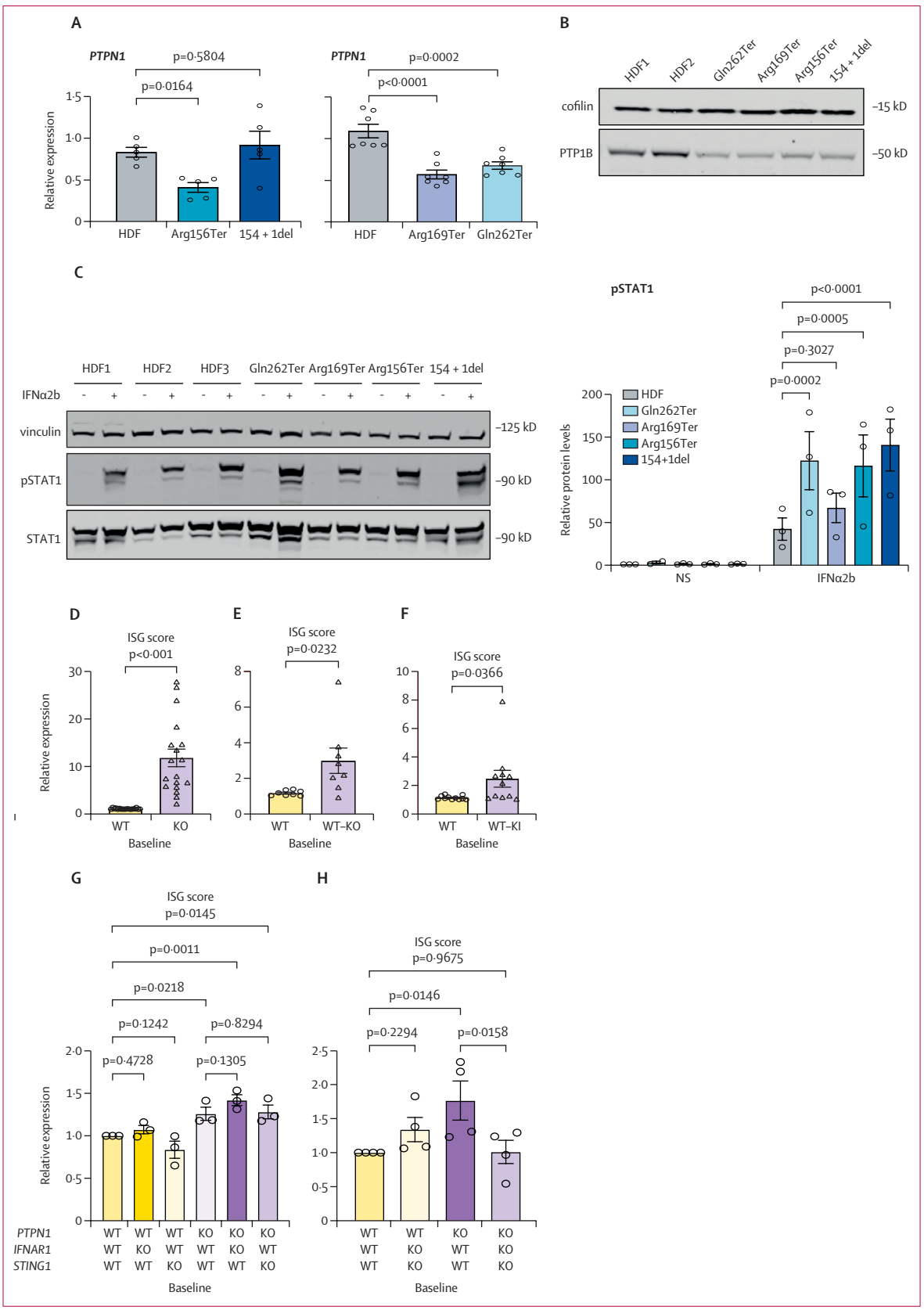
A
PTPN1
p=0·5804
p=0·0164
Relative expression
HDF
Arg156Ter
154 + 1del
PTPN1
p=0·0002
p<0·0001
HDF
Arg169Ter
Gln262Ter
B
HDF1
HDF2
Gln262Ter
Arg169Ter
Arg156Ter
154 + 1del
cofilin
–15 kD
PTP1B
–50 kD
C
HDF1
HDF2
HDF3
Gln262Ter
Arg169Ter
Arg156Ter
154 + 1del
IFNα2b
vinculin
–125 kD
pSTAT1
–90 kD
STAT1
–90 kD
pSTAT1
p<0·0001
p=0·0005
p=0·3027
p=0·0002
HDF
Gln262Ter
Arg169Ter
Arg156Ter
154+1del
Relative protein levels
NS
IFNα2b
D
ISG score
p<0·001
Relative expression
WT
KO
Baseline
E
ISG score
p=0·0232
WT
WT–KO
Baseline
F
ISG score
p=0·0366
WT
WT–KI
Baseline
G
ISG score
p=0·0145
p=0·0011
p=0·0218
p=0·1242
p=0·8294
p=0·4728
p=0·1305
Relative expression
PTPN1
IFNAR1
STING1
Baseline
H
ISG score
p=0·9675
p=0·0146
p=0·2294
p=0·0158
Baseline

function and type 1 IFN signalling was investigated in vitro. Using CRISPR–Cas9 gene editing in BJ-5ta human fibroblasts (an hTERT immortalised cell line commonly employed in studies of innate immune sensing and type 1 IFN signalling), *PTPN1* homozygous knockout single-cell clones were generated (appendix p 16). These cells demonstrated significantly enhanced ISG expression at baseline compared with wildtype control cells, assessed both by targeted qPCR (figure 4D) and by bulk RNA sequencing (appendix p 16). Given that haploinsufficiency was considered to be the probable molecular mechanism underlying the disease in this patient cohort, heterozygous wildtype knockout (WT-KO) BJ-5ta clones were also generated, as well as a clone wildtype heterozygous knock-in (WT-KI) for the canonical donor splice site 63+1G→C variant seen in AGS761 (which leads to a splicing defect and loss of mRNA expression). As expected, and similar to results in patient primary fibroblasts, WT-KO and WT-KI cells displayed intermediate levels of PTP1B expression (appendix p 16). Similar to complete *PTPN1* knockout cells, albeit to a lesser degree, WT-KO (figure 4E) and WT-KI (figure 4F) heterozygous clones exhibited elevated baseline ISG expression compared to wildtype controls, suggesting enhanced IFN signalling.

PTP1B has been implicated in the dephosphorylation of TYK2, a component of the ubiquitously expressed type 1 IFN receptor (IFNAR) complex, and in the degradation of STING (encoded by *STING1*), an adaptor protein central to cytosolic DNA sensing, both of which could lead to enhanced type 1 IFN signalling at baseline and on stimulation (appendix p 16). Notably, *PTPN1*-deficient cells demonstrated higher global phosphotyrosine protein levels even at baseline (appendix p 16), indicative of a general failure of phosphatase activity. STING levels were also higher in unstimulated *PTPN1* knockout cells (appendix p 17). Thus, to further explore the negative regulation of type 1 IFN signalling by PTP1B, *PTPN1* wildtype, knockout, WT-KO, and WT-KI BJ-5ta cells were stimulated with either IFNα2b or the STING agonist diABZI. Significantly increased IFN signalling was detected after both IFNα2b and diABZI stimulation, as shown by the measurement of global phosphotyrosine protein levels (appendix p 16), ISG expression (appendix p 17) and p-STAT1 (appendix p 17). Consistently, *PTPN1* WT-KO and WT-KI clones also demonstrated increased ISG expression following IFNα2b and diABZI stimulation (appendix p 17). Of note, phosphorylated STING (p-STING) protein and *IFNB1* mRNA levels were also induced at a higher level on diABZI stimulation, suggesting enhanced sensitivity of the STING pathway upstream of IFNAR signalling (appendix p 17).

To distinguish the effects of *PTPN1* deficiency on IFNAR and STING activity, *STING1* knockout and *IFNAR1* knockout cell pools were generated on a *PTPN1* wildtype or knockout background in hTERT-immortalised RPE-1 cells (appendix p 18), in which ISG upregulation was also observed in the absence of PTP1B (appendix p 18). RPE-1 cells are also commonly used in innate immune sensing studies, and this alternative cell line was employed since BJ-5ta fibroblasts were found to be intolerant of multiple rounds of CRISPR gene editing. Western blot confirmed successful knockout of *STING1* and *IFNAR1* in *PTPN1* wildtype and knockout cells (appendix p 18). Assessing baseline ISG expression in these double-knockout cell lines indicated that neither *IFNAR1* nor *STING* knockout alone rescued the enhanced ISG expression seen in *PTPN1*-deficient cells (figure 4G). By contrast, with combined deletion of *IFNAR1* and *STING1*, ISG expression levels were equivalent to those seen in *PTPN1* wildtype cells (figure 4H), consistent with an effect of PTP1B on both IFNAR1 and STING function.

Discussion

In this study, we identified 12 patients from 11 families harbouring one of ten distinct novel or very rare heterozygous mutations in *PTPN1*, with a variant occurring de novo in three individuals. Six of these variants introduced premature stop codons and two involved canonical donor splice-site nucleotides that were predicted to result in abnormal splicing. These variants were shown to be loss of function, noting that *PTPN1* is a highly constrained gene intolerant of null variants (with <40 of about 750 000 individuals harbouring such variants annotated on gnomAD version 4.1.0). Further, both missense variants identified by us have been shown previously to be important in the allosteric regulation of PTP1B activity.[20,21] Finally, we observed the same Arg156Ter mutation (not present on more than 1 600 000 alleles recorded in gnomAD version 4.1.0) in two unrelated patients, in one of whom the variant occurred de novo. Given these molecular data, we are confident that haploinsufficiency for *PTPN1* represents a novel human mendelian disease.

It is of note that we also identified nine asymptomatic and mutation-positive family members of the symptomatic patients. The deleterious or protective effect of other genetic variants, epigenetic modifications, and environmental factors might all affect disease penetrance and expressivity, with clinical non-penetrance an increasingly recognised phenomenon in mendelian disorders in general,[22] and immunological diseases in particular.[23] Notably, clinical non-penetrance has been described in both autosomal dominant and recessive mutant genotypes associated with enhanced type 1 IFN signalling.[16,24,25] Further, three such instances of clinical non-penetrance were reported in the context of autosomal dominant *PTPN2* loss-of-function mutations.[13] At this time, we cannot rule out the possibility that clinically asymptomatic individuals are at risk of disease in later life (or that patients affected during childhood might experience recurrent episodes of loss of skills). Finally, we note that two of the variants that we observed have been described as somatic driver mutations in B-cell

lymphomas.[5] We did not record any cancers in the cohort of individuals that we ascertained, and there was no family history of such. However, this observation should be kept in mind during the long-term follow-up of affected individuals and their clinically asymptomatic mutation-positive relatives.

The phenotype of the 12 patients described here is remarkably stereotyped, being characterised by subacute loss of skills following initially normal development, spastic dystonia, bulbar involvement, preserved head circumference, and an absence of seizures. Seven patients were noted to demonstrate an asymmetry of clinical signs at initial presentation, and in four of these individuals, there was asymmetry of the cerebral atrophy that was seen on neuroimaging in nine of 12 patients overall. In the context of such asymmetry, the absence of seizures is notable in differentiating this disease from Rasmussen encephalitis, whereas the absence of neuropsychiatric features, and negative testing for neural antibodies in seven patients, also distinguishes the novel disorder that we describe from antibody-mediated encephalitis.

The observation of enhanced type 1 IFN signalling in patient blood and CSF, and of increased levels of CSF neopterin,[26,27] suggests that *PTPN1* haploinsufficiency can be classified as a novel type 1 interferonopathy.[28] Indeed, the paradigm type 1 interferonopathy Aicardi-Goutières syndrome was considered as a possible diagnosis in several of the cases described here. Although Aicardi-Goutières syndrome classically presents in the first year of life with white-matter involvement, intracranial calcification, and cerebral atrophy, cases with a later onset and normal neuroimaging or non-specific white-matter changes, with or without intracranial calcification, are well described. Features apparently distinguishing PTP1B-related encephalopathy from Aicardi-Goutières syndrome are a later age at onset (nine of 12 cases in our cohort presenting beyond 18 months of age), notable bulbar involvement manifesting as difficulties with swallowing and expressive speech, and cerebral atrophy as the predominant neuroradiological sign.

Considering the probable inflammatory basis of Aicardi-Goutières syndrome, a few reports have described the use of broad-spectrum immunosuppression in affected individuals,[29,30] without obvious clinical efficacy. By contrast, in six of eight treated cases described here, it was judged clinically that neurological status improved in association with high-dose corticosteroids (with or without intravenous immunoglobulin, azathioprine, and mycophenolate mofetil, including three patients previously reported by Sa and colleagues,[14] all of whom were found to harbour mutations in *PTPN1* in this study). However, it is also the case that all 12 patients demonstrated clinical stabilisation, even if most were left with major neurological deficits, and there was complete or near-complete resolution of the cerebral atrophy and white-matter disease seen in the initial stages of the disease, irrespective of treatment status. Thus, the precise relationship of steroid therapy to clinical outcome in *PTPN1* haploinsufficiency remains uncertain. Again, relating to treatment, a possible clinical implication of our work would be to use JAK1 and TYK2 inhibition as a therapeutic strategy (with JAK1 and TYK2 components of the type 1 IFN receptor complex). To our knowledge, no patients with haploinsufficiency of *PTPN1* have yet been treated in this way. One possible difficulty with this approach would be the known limited penetration of such drugs into the CNS.

In a high-throughput screening assay involving gene silencing in mouse embryonic fibroblasts, with follow-up experiments in human monocyte-derived dendritic cells, PTP1B was identified as a negative regulator of type 1 IFN signalling after DNA stimulation.[6] Several possible mechanisms have been suggested to account for this negative regulatory function of PTP1B, including through roles in TYK2 dephosphorylation and STING proteasomal degradation.[7,8] Our patient and in-vitro data emphasise the importance of PTP1B in the control of STING and JAK-STAT signalling in human immune homoeostasis.[3] By extrapolation, given that PTP1B inhibitors are in active development for a variety of indications,[2] our findings indicate a need for careful neurological monitoring with the use of such inhibition.

The present study is limited by the relatively small number of patients ascertained and the retrospective nature of the analysis. The identification of more patients will provide important information on the breadth of phenotype associated with *PTPN1* haploinsufficiency, and a better understanding of the appropriate management and treatment of this disorder. Prospective follow-up will also provide new knowledge on the risk, if any, of further episodes of neurological loss of skills and other phenotypes (particularly myeloma) in symptomatic patients, and of individuals asymptomatic into adulthood manifesting later-onset disease.

Contributors

GZ was responsible for data curation, formal analysis, investigation, methodology, software, validation, visualisation, writing of the original draft, and reviewing and editing the manuscript. YJC did the conceptualisation, data curation, formal analysis, funding acquisition, investigation, methodology, project administration, supervision, validation, visualisation, writing of the original draft, and reviewing and editing the manuscript. M-TE-D did the conceptualisation, data curation, formal analysis, methodology, supervision, validation, visualisation, and reviewing and editing the manuscript. AL did the conceptualisation, data curation, formal analysis, funding acquisition, investigation, methodology, project administration, supervision, validation, visualisation, writing of the original draft, and reviewing and editing of the manuscript. VB was responsible for the methodology, investigation, and reviewing and editing of the manuscript. BA did the investigation and data collection. AS was responsible for data acquisition and interpretation. MK did the investigation and reviewing and editing of the manuscript. All other authors contributed to the investigation. All authors reviewed the manuscript. GZ, YJC, M-TE-D, and AL had access

to and verified the original unprocessed in-vitro experimental data. All authors had access to and verified the clinical and in-vitro experimental data presented in the manuscript. All authors agreed to submit the manuscript.

Declaration of interests

TG reports a grant for the impact of anti-viral immunity in solid organ transplantation: mechanisms of host infection control in immunosuppressed and infection-prone individuals (TTU07.822_00) from Deutsches Zentrum für Infektionsforschung. OBT receives payment from HCERES (the French Scientific Authority), HAS (the French Health Authority), Italfarmaco, and Minoryx for expert testimony. OBT serves on the Data and Safety Monitoring Board for Minoryx and as the unpaid Scientific Council President of AFM Telethon. YH receives grants from Great Ormond Street Hospital (GOSH) Children Charity and MS Society UK, honoraria from the AAN Continuum, and has served unpaid roles in the Neurology Journal Editorial Board, the MS Society UK Advisory Group for Medications, the MOG Project Medical Advisory Board, and the Guthy-Jackson Foundation International Clinical Consortium. ML has received the following grants: the minimal motion system for MRI: MR-MinMo (Clinical Lead) from the National Institute for Health and Care Research (NIHR204201); multimodal assessment of remyelination and light-chain neurofilament assay following demyelination episodes in children (MARMALADE-C; Doctoral supervision) from Action Medical Research (GN2945); investigating the neurological impact of COVID-19 in non-hospitalised children with persistent symptoms (Clinical Lead) from Action Medical Research (GN2925); validation of the paediatric autoimmune encephalitis severity score (PASS) in children with autoimmune encephalitis (clinical supervision) from the Encephalitis Society; prognosis, treatment, and mechanisms in an international paediatric-onset opsoclonus myoclonus ataxia syndrome study (POOMAS; UK Lead) from the Boston Children's Hospital Research Fund (GENFD0001772273); developing magnetic resonance measures of neurobiological dysfunction in early recovery from NMDAR-antibody encephalitis (Doctoral Supervisor) from Action Medical Research (GN2835); and long-term sequelae following PIM-TS (study co-lead) from GOSH Charity Rapid Response Funding Call (VC1421). ML has received consulting fees from Roche, Novartis, and Octapharma as part of the respective Expert Advisory Board. ML gives around four lectures, presentations, and meetings per year and all honoraria are paid to ML's institutional research account. ML performs up to six medical legal cases a year, and serves as data monitoring committee Chair in the AGSRTI Trial evaluating reverse transcriptase inhibition as treatment in Aicardi-Goutières syndrome (NCT04731103). ML serves as on the steering committee in the phase III study to compare the effect of panzyga versus placebo in patients with paediatric acute-onset neuropsychiatric syndrome (NCT04508530), as unpaid co-Chair of the European Paediatric Neurology Society Education and Training Board, as unpaid co-Chair of the James Lind Alliance and British Paediatric Neurology Association Research Priority Setting Partnership, and has a paid leadership role as Associate Editor of the European Journal of Paediatric Neurology. MMM receives payment from Jazz Pharmaceuticals and serves on the Advisory Board of Italfarmaco. IM receives payments from Boehringer Ingelheim and GSK, and support for travel and meetings from Novartis. All other authors declare no competing interests.

Data sharing

Exome sequencing data are not publicly available due to the possibility of compromising privacy. Human fibroblasts are primary cells and therefore a limited resource. Availability is through the corresponding authors subject to technical constraints and completion of a material transfer agreement required to ensure patient privacy.

Acknowledgments

YJC acknowledges the European Research Council (786142 E-T1IFNs), a UK Medical Research Council Human Genetics Unit core grant (MC_UU_00035/11), a state subsidy from the Agence Nationale de la Recherche (France) under the Investissements d'Avenir programme, bearing the reference ANR-10-IAHU-01, and funding from the Agence Nationale de la Recherche for the Phospho-IFN project (ANR-24-CE15-4638). GZ is funded by the European Union's Horizon 2020 research and innovation programme under the Marie Skłodowska-Curie grant agreement 955576. MH, ZS, and MV acknowledge grant NU22-07-00165 from the Czech Ministry of Health.

References

1 Tonks NK. Protein tyrosine phosphatases: from genes, to function, to disease. *Nat Rev Mol Cell Biol* 2006; **7:** 833–46.
2 Stanford SM, Bottini N. Targeting protein phosphatases in cancer immunotherapy and autoimmune disorders. *Nat Rev Drug Discov* 2023; **22:** 273–94.
3 Read NE, Wilson HM. Recent developments in the role of protein tyrosine phosphatase 1B (PTP1B) as a regulator of immune cell signalling in health and disease. *Int J Mol Sci* 2024; **25:** 7207.
4 Elchebly M, Payette P, Michaliszyn E, et al. Increased insulin sensitivity and obesity resistance in mice lacking the protein tyrosine phosphatase-1B gene. *Science* 1999; **283:** 1544–48.
5 Gunawardana J, Chan FC, Telenius A, et al. Recurrent somatic mutations of PTPN1 in primary mediastinal B cell lymphoma and Hodgkin lymphoma. *Nat Genet* 2014; **46:** 329–35.
6 Lee MN, Roy M, Ong SE, et al. Identification of regulators of the innate immune response to cytosolic DNA and retroviral infection by an integrative approach. *Nat Immunol* 2013; **14:** 179–85.
7 Myers MP, Andersen JN, Cheng A, et al. TYK2 and JAK2 are substrates of protein-tyrosine phosphatase 1B. *J Biol Chem* 2001; **276:** 47771–74.
8 Xia T, Yi XM, Wu X, Shang J, Shu HB. PTPN1/2-mediated dephosphorylation of MITA/STING promotes its 20S proteasomal degradation and attenuates innate antiviral response. *Proc Natl Acad Sci USA* 2019; **116:** 20063–69.
9 Bourdeau A, Dubé N, Tremblay ML. Cytoplasmic protein tyrosine phosphatases, regulation and function: the roles of PTP1B and TC-PTP. *Curr Opin Cell Biol* 2005; **17:** 203–09.
10 Parlato M, Nian Q, Charbit-Henrion F, et al, and the Immunobiota Study Group. Loss-of-function mutation in PTPN2 causes aberrant activation of JAK signaling via STAT and very early onset intestinal inflammation. *Gastroenterology* 2020; **159:** 1968–71.
11 Awwad J, Souaid M, Yammine T, et al. A homozygous missense variant in *PTPN2* with early-onset Crohn's disease, growth failure and dysmorphic features in an infant: a case report. *J Genet* 2023; **102:** 102.
12 Thaventhiran JED, Lango Allen H, Burren OS, the Primary Immunodeficiency Consortium for the NIHR Bioresource. Whole-genome sequencing of a sporadic primary immunodeficiency cohort. *Nature* 2020; **583:** 90–95.
13 Jeanpierre M, Cognard J, Tusseau M, et al. Haploinsufficiency in PTPN2 leads to early-onset systemic autoimmunity from Evans syndrome to lupus. *J Exp Med* 2024; **221:** e20232337.
14 Sa M, Hacohen Y, Alderson L, et al. Immunotherapy-responsive childhood neurodegeneration with systemic and central nervous system inflammation. *Eur J Paediatr Neurol* 2018; **22:** 882–88.
15 Rice GI, Forte GM, Szynkiewicz M, et al. Assessment of interferon-related biomarkers in Aicardi-Goutières syndrome associated with mutations in TREX1, RNASEH2A, RNASEH2B, RNASEH2C, SAMHD1, and ADAR: a case-control study. *Lancet Neurol* 2013; **12:** 1159–69.
16 Lepelley A, Martin-Niclós MJ, Le Bihan M, et al. Mutations in COPA lead to abnormal trafficking of STING to the Golgi and interferon signaling. *J Exp Med* 2020; **217:** e20200600.
17 Rodero MP, Decalf J, Bondet V, et al. Detection of interferon alpha protein reveals differential levels and cellular sources in disease. *J Exp Med* 2017; **214:** 1547–55.
18 Lebon P, Badoual J, Ponsot G, Goutières F, Hémeury-Cukier F, Aicardi J. Intrathecal synthesis of interferon-alpha in infants with progressive familial encephalopathy. *J Neurol Sci* 1988; **84:** 201–08.
19 Sa M, Hacohen Y, Alderson L, et al. Immunotherapy-responsive childhood neurodegeneration with systemic and central nervous system inflammation. *Eur J Paediatr Neurol* 2018; **22:** 882–88.
20 Keedy DA, Hill ZB, Biel JT, et al. An expanded allosteric network in PTP1B by multitemperature crystallography, fragment screening, and covalent tethering. *eLife* 2018; **7:** 7.
21 Hjortness MK, Riccardi L, Hongdusit A, et al. Evolutionarily conserved allosteric communication in protein tyrosine phosphatases. *Biochemistry* 2018; **57:** 6443–51.

22 Kingdom R, Wright CF. Incomplete penetrance and variable expressivity: from clinical studies to population cohorts. *Front Genet* 2022; **13:** 920390.

23 Gruber C, Bogunovic D. Incomplete penetrance in primary immunodeficiency: a skeleton in the closet. *Hum Genet* 2020; **139:** 745–57.

24 Rice GI, Park S, Gavazzi F, et al. Genetic and phenotypic spectrum associated with IFIH1 gain-of-function. *Hum Mutat* 2020; **41:** 837–49.

25 Crow YJ, Gonzalez-Granado LI, Coarelli G, the AGS group. Clinical non-penetrance associated with biallelic mutations in the rNase H2 complex. *J Clin Immunol* 2023; **43:** 706–08.

26 Dale RC, Brilot F, Fagan E, Earl J. Cerebrospinal fluid neopterin in paediatric neurology: a marker of active central nervous system inflammation. *Dev Med Child Neurol* 2009; **51:** 317–23.

27 Han VX, Mohammad SS, Jones HF, Bandodkar S, Crow YJ, Dale RC, the AGS-JAKi Study Group. Cerebrospinal fluid neopterin as a biomarker of treatment response to Janus kinase inhibition in Aicardi-Goutières syndrome. *Dev Med Child Neurol* 2022; **64:** 266–71.

28 Crow YJ, Casanova JL. Human life within a narrow range: The lethal ups and downs of type I interferons. *Sci Immunol* 2024; **9:** eadm8185.

29 Orcesi S, Pessagno A, Biancheri R, et al. Aicardi-Goutières syndrome presenting atypically as a sub-acute leukoencephalopathy. *Eur J Paediatr Neurol* 2008; **12:** 408–11.

30 D'Arrigo S, Riva D, Bulgheroni S, et al. Aicardi-Goutières syndrome: description of a late onset case. *Dev Med Child Neurol* 2008; **50:** 631–34.